Theoret. Comput. Fluid Dynamics (2001) 15: 65–81

**Theoretical and Computational Fluid Dynamics**



# Optimal Control of Nonmodal Disturbances in Boundary Layers

**Peter Corbett*** **and Alessandro Bottaro**

Institut de Mécanique des Fluides de Toulouse,
Allée du Pr. Camille Soula,
31400 Toulouse, France

Communicated by T.B. Gatski

Received 5 February 2001 and accepted 15 June 2001

**Abstract.** The optimal control of infinitesimal flow disturbances experiencing the largest transient gain over a fixed time span, commonly termed "optimal perturbations," is undertaken using a variational technique in two- and three-dimensional boundary layer flows. The cost function employed includes various energy metrics which can be weighted according to their perceived importance, simplifying the task of determining which terms are essential for a "good" control scheme. In the accelerated boundary layers investigated, disturbance kinetic energy can be typically reduced by about one order of magnitude. However, it seems impossible to suppress perturbations completely over the entire control interval; "good" control strategies still permit approximately an order of magnitude growth over the initial energy at some point in the interval. It is shown that the control effort efficiently targets the physical mechanisms behind transient growth.

## 1. Introduction

Flow control has long fascinated humankind. Irrigation for agricultural purposes, perhaps the most widespread form of flow control, is thought to have been invented about nine millennia ago; there is a case for arguing that modern civilization is a direct consequence of this technology. More recently, the problem of determining the form an axisymmetric body should take in order to move through air with the least resistance, an implicit form of flow control, inspired Newton to lay the foundations of the calculus of variations. Prandtl's seminal work on boundary layers at the beginning of the last century also proposed techniques for controlling their separation. This report describes the control of small perturbations in boundary layers using a variational approach.

Air travel is now a pervasive feature of modern life, as a consequence improvements in aircraft performance are avidly sought. One such possibility lies in bettering the craft's aerodynamics, with the specific objective of minimizing viscous drag, which offers about half the total resistance to motion. While viscous drag is unavoidable, at a given Reynolds number, laminar skin friction can be up to 90% *less* than turbulent skin friction (Joslin, 1998). In practical terms, this implies that methods must be found for delaying the onset of the transition from laminar to turbulent flow, a process which continues to elude complete understanding.

* This work began while PC was at the Laboratoire de Mécanique des Fluides, École Polytechnique Fédérale de Lausanne, 1015 Lausanne, Switzerland, where he was partially supported by Swiss National Science Foundation Grant 2100–52'592.97.

The classical theory describing transition is due to Prandtl and his students. In it, environmental disturbances excite two-dimensional waves inside the boundary layer which are exponentially amplified. These Tollmien–Schlichting (TS) waves quickly manifest spanwise variations, giving rise to complex three-dimensional motions which are the precursors to turbulence. Until recently, the attention of workers seeking to understand transition has focused upon these two-dimensional waves.

In his reviews of the flow control problem, Gad-el-Hak (1989, 1996) makes a distinction between two methods for transition control. Stability modifiers seek to change the shape of the mean flow velocity profile and hence its stability characteristics. Wave cancellation targets the linear disturbances directly, exploiting but not changing the stability properties of the mean flow. The latter technique is applicable while the perturbation is small and the principle of linear superposition still holds. Its principal advantage is in the energetics: presumably less effort is required to subdue or modify infinitesimal disturbances than to change the mean boundary layer. Below, a small selection of the relevant prior work on the direct active control of flow instabilities is reviewed (for a comprehensive review, see Joslin *et al.* (1997)).

Wave cancellation has been essayed in physical and numerical experiments. In an early experiment, Milling (1981) demonstrated the viability of the approach in a water tunnel by exciting TS waves using a vibrating ribbon at one station on a flat plate. Another wave, 180° out of phase with respect to the first, was introduced at a downstream station by identical means and the resulting wave cancellation caused the transition location to move beyond the plate's end. In other early work, Biringen (1984) used temporal direct numerical simulation (DNS) to study the efficacy of periodic suction/blowing as a control mechanism in plane channel flow. Reduction in the amplitude and growth rate of relatively large TS waves was attained by control applied over one time step. Bower *et al.* (1987) confirmed the efficacy of wave cancellation for two-dimensional disturbances in the context of the Orr–Sommerfeld equation, showing that such waves could be attenuated via blowing/suction at the wall. In a more detailed DNS study, Laurien and Kleiser (1989) investigated the control of waves in boundary layers via two-dimensional blowing/suction at the wall over a finite time span. They reported up to an order of magnitude decrease in disturbance amplitude with subsequent transition delay when the control was applied early in the process, but noted that streamwise vortices already present in the flow were unaffected by this type of control. Experimental confirmation of the feasibility of control via blowing/suction was provided by Ladd (1990), who used an "invert & delay" feedback controller to stabilize the naturally occurring flow about a slender ellipsoid. In this experiment, the wall shear stress was halved. Breuer *et al.* (1989) applied a similar approach to the control of small- and large-amplitude transient disturbances in a boundary layer, using the deformation of flexible membranes mounted flush to the wall to induce control flow. By tuning the time delay between the actuation of the disturbance seeder and a series of control membranes they were able to postpone the disturbances' breakdown into a turbulent spot by about $50\,\delta^*$.

The last decade has seen a marked increase in the application of sophisticated mathematical techniques to the active control of flow disturbances. Abergel and Témam (1990) applied the rigorous theoretical framework afforded by the theory of optimal control to the problem of controlling turbulence in some simple two-dimensional configurations. This approach was later adopted by Joslin *et al.* (1997), who applied it to the suppression of a TS wave by suction/blowing at the wall in the context of a two-dimensional DNS. Bewley and Liu (1998) used modern control theoretical techniques to determine optimal and robust controllers for linear waves and nonmodal disturbances in plane channel flows, also utilizing suction/blowing at the wall. This approach is particularly relevant for practical implementation of stable closed-loop controllers as might be envisioned in aerospace applications. Cathalifaud and Luchini (2000) attacked the problem of controlling linear optimal perturbations in spatially developing boundary layers on flat and concave plates by considering the wall receptivity. They used a direct/adjoint method to demonstrate that it was possible to annihilate completely the streamwise disturbance at a given downstream position, although the control provoked a larger transient gain than that experienced by the uncontrolled perturbation. The use of adjoint techniques for boundary layer receptivity studies was initiated by Hill (1995), who employed it to gauge the effect of various sorts of forcing on the flow.

The optimal perturbations referred to above are the result of some recent developments in the field of hydrodynamic stability. It has been shown that suitably configured infinitesimal disruptions can grow by many orders of magnitude, even in subcritical flows (Butler and Farrell, 1992; Trefethen *et al.*, 1993; Luchini, 2000). These perturbations take the form of vortices aligned with the mean flow, they engender streaks (large variations in the streamwise perturbation velocity, commonly observed in experiments on transitional flows)

and must be considered in any attempt to engineer flows with large laminar regions, since they may prematurely initiate transition. Control is of particular relevance for three-dimensional flows, not only since these tend to be more prevalent in engineering applications, but also because the optimal initial disturbance in this family of flows feeds the strongly growing exponential crossflow instability (Corbett and Bottaro. 2001). Since optimal perturbations are non-modal in nature, the wave cancellation techniques based on mode superposition previously explored in the literature are not readily applicable, and optimal control theory suggests itself.

The objective here is to control the growth of optimal perturbations in subcritical two- and three-dimensional boundary layers via suction and blowing at the wall, as has been shown to be feasible for TS waves. The perturbations evolve in time in a "frozen" or parallel boundary layer, the goal is to determine the time-varying wall-normal velocity at the wall which best attenuates them. The control targets the disturbances directly, since this demands less control effort. Clearly, if the control requires more energy than would be otherwise consumed in overcoming increased drag due to turbulence, it is economically uninteresting. The variational method employed to determine the optimal distribution of suction and blowing at the wall is described, and the physical mechanisms exploited by the control are discussed for several practically relevant cases.

The temporal approximation is unphysical for this class of problems; it has been employed here because it leads to a relatively straightforward optimality system. Unfortunately, there is no correspondingly straightforward manner of transforming the results into the spatial framework, unlike classical linear stability theory (Gaster, 1962; Nayfeh and Padhye, 1979; Nayfeh, 1980). Further, while direct simulations (which are perhaps the best yardstick with which to compare nonmodal results) indicate that results obtained using the temporal approach may be mapped with fair accuracy into a spatial context (Laurien and Kleiser, 1989; Breuer and Kuraishi, 1994; Lasseigne *et al.*, 1999), the full extension of this work into the spatial context is by no means trivial: for three-dimensional flows the perturbation should be tracked from the attachment-line. Finally, this linear analysis is unable to account for eventual nonlinear interactions between the control and the disturbance. Clearly, the present work must be viewed as preliminary and exploratory in nature, and the findings and control laws reported can only be interpreted qualitatively.

## 2. Model System

The behavior of small, unsteady, three-dimensional perturbations, $\tilde{\boldsymbol{u}}(x, y, z, t) = (\tilde{u}, \tilde{v}, \tilde{w}, \tilde{p})^{\mathrm{T}}$, is considered as they evolve in the base flow under consideration. In the temporal approach used here, the base flow is assumed to be parallel, taking the form $\boldsymbol{U} = (U(y), 0, W(y), P(x))^{\mathrm{T}}$. The Navier–Stokes equations are then written for $\hat{\boldsymbol{u}}(x, y, z, t) = \boldsymbol{U} + \tilde{\boldsymbol{u}}$. Since disturbances are small the equations may be linearized about the base flow and the resulting system used to study the perturbation.

### 2.1. Base Flow

For generality, the two-parameter family of similarity solutions for yawed wedge flows given by Cooke (1950) is used to specify the base flow. One parameter, $m$, communicates the intensity of the pressure gradient, the other is the yaw (or sweep) angle $\Lambda$, specifying the ratio of chord- to spanwise velocities in the undisturbed external flow. On the one hand, with both parameters zero this model recovers the Blasius boundary layer, whereas on the other it can also be used to model the three-dimensional accelerated flow occurring on an infinite swept wing.

The general situation is shown in Figure 1(a), where the wedge coordinate system (subscript "w") is such that $x_{\mathrm{w}}$ lies perpendicular to the wedge leading edge, $z_{\mathrm{w}}$ lies along it, and $y$ is normal to the surface. The corresponding velocity components inside the boundary layer are $U_{\mathrm{w}}$, $W_{\mathrm{w}}$, and $V$. Using the Blasius similarity variable $\xi = \sqrt{U_{\mathrm{e}}/(\nu x_{\mathrm{w}})}\, y$, an affine solution to the boundary layer equations is sought for the case where $U_{\mathrm{e}} = C x_{\mathrm{w}}^m$ and $W_{\mathrm{e}} = \text{constant}$, the subscript "e" indicating the situation external to the boundary layer at the chordwise position under consideration. Introducing a stream function of the form $\psi = \sqrt{U_{\mathrm{e}} \nu x_{\mathrm{w}}}\, f(\xi)$, continuity is satisfied directly and as a result $U_{\mathrm{w}} = U_{\mathrm{e}}\, \mathrm{d}f/\mathrm{d}\xi$. Assuming $W_{\mathrm{w}} = W_{\mathrm{e}} g(\xi)$, the momentum equations

**Table 1.** Boundary layer quantities and optimal perturbation parameters for flow at $R_\theta = 166$, $m = 0.1$. $\Gamma$ indicates the growth attained by the optimal disturbance over the span $t = t_\Gamma$.

| $\phi$ | $\delta^*$ | $\theta$ | $\alpha_\theta$ | $\beta_\theta$ | $\Gamma$ | $t_\Gamma$ |
|---|---|---|---|---|---|---|
| 0° | 1.3478 | 0.5566 | 0 | 0.2522 | 227.4 | 863.5 |
| 45° | 1.4444 | 0.5806 | 0.0140 | 0.2312 | 360.0 | 616.0 |

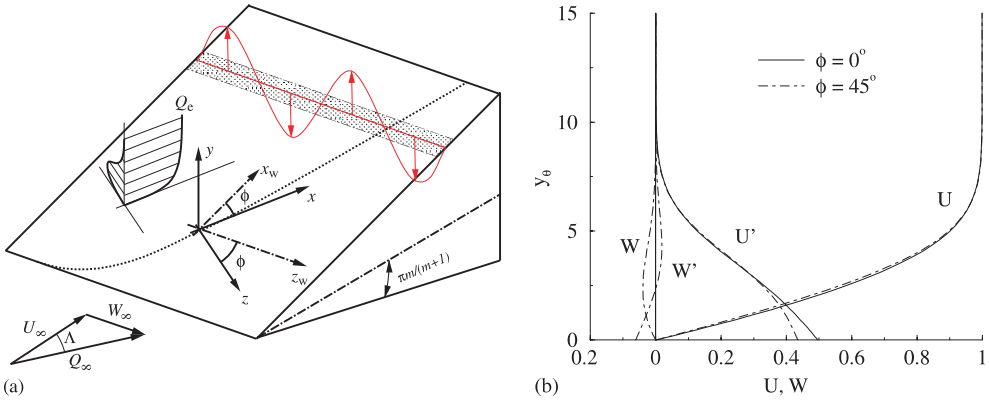


**Figure 1.** (a) Sketch of the problem laying out the reference system and illustrating the mean flow. As shown, control is through slots, with the indicated wall-normal velocity applied at the wall only in the shaded region. (b) Falkner–Skan–Cooke solutions for $m = 0.1$ at various sweep angles. At 45° maximum cross-flow occurs.

then yield the system

$$f''' + \frac{m+1}{2} f f'' + m(1 - f'^2) = 0,$$
$$g'' + \frac{m+1}{2} f g' = 0,$$
$$f(0) = f'(0) = g(0) = 0 \quad \text{and} \quad f'(\infty) = g(\infty) = 1,$$

where primes indicate derivatives with respect to the independent variable.

After Gregory *et al.* (1955), flow stability is studied in the frame of reference of the external streamline. If $\phi$ is the angle between the reference frame aligned with the external potential flow and the wing coordinate system, and assuming $\Lambda \approx \phi$, as might be expected some distance from the leading edge, the velocity components parallel and normal to the external flow are given by

$$U(\xi) = f'(\xi)\cos^2\phi + g(\xi)\sin^2\phi,$$
$$W(\xi) = [g(\xi) - f'(\xi)]\cos\phi\sin\phi,$$

when nondimensionalized with respect to $Q_e$. Figure 1(b) shows the velocity profiles corresponding to the flows investigated here. All reference lengths are defined with respect to the momentum thickness based on the streamwise component of the mean flow, given by $\theta = \int_0^\infty U\,(1-U)\,\mathrm{d}\xi$, and listed in Table 1. Aside from time $t$, dependent quantities are indicated by a subscript $\theta$.

### 2.2. Small Perturbations

The system of linearized Navier–Stokes equations mentioned previously is customarily reduced to two equations. First the perturbation pressure is eliminated, then the $x$- and $z$-momentum equations are combined to form an expression for the perturbation vorticity in the wall-normal sense,

$$\tilde{\eta} = \frac{\partial \tilde{u}}{\partial z} - \frac{\partial \tilde{w}}{\partial x}\,.$$

The disturbance is then completely described by $\tilde{\boldsymbol{v}} = (\tilde{v}, \tilde{\eta})^{\mathrm{T}}$. Assuming spatial periodicity in the stream- and spanwise directions,

$$\tilde{\boldsymbol{v}}(x, y, z, t) = \boldsymbol{v}(y, t) \exp(\mathrm{i}\alpha x + \mathrm{i}\beta z)$$

with $\alpha$ and $\beta$ the corresponding (real) wavenumbers, results in the following system for $\boldsymbol{v}$:

$$\mathsf{F}\boldsymbol{v} = 0, \quad \text{where} \quad \mathsf{F} = \mathsf{I}\frac{\partial}{\partial t} + \Lambda. \tag{1}$$

Here $\mathsf{I}$ is the identity matrix, and

$$\Lambda = \begin{bmatrix} \Delta^{-1}(\mathsf{C}\Delta - \mathrm{i}\alpha U'' - \mathrm{i}\beta W'') & 0 \\ -\mathrm{i}\alpha W' + \mathrm{i}\beta U' & \mathsf{C} \end{bmatrix}, \qquad \text{with} \quad \mathsf{C} = \mathrm{i}\alpha U + \mathrm{i}\beta W - \frac{1}{R}\Delta.$$

The Laplacian operator is represented above by $\Delta = \partial^2/\partial y^2 - k^2$, with $k^2 = \alpha^2 + \beta^2$. The Reynolds number

$$R = \frac{Q_{\mathrm{e}}\delta}{\nu},$$

characterizing the relative importance of convective to diffusive processes, appears when the original system is uniformly nondimensionalized using a characteristic length ($\delta$) and velocity ($Q_{\mathrm{e}}$). Pressure is scaled by the grouping $\rho Q_{\mathrm{e}}^2$ and $\delta$ is taken to be proportional to the boundary layer thickness, $\delta = \sqrt{\nu\ell/Q_{\mathrm{e}}}$, where $\ell$ is a reference distance in the chordwise sense.

Boundary conditions on the normal perturbation velocity, its normal derivative, and the perturbation vorticity are necessary to render (1) well posed. Since disturbances are assumed to vanish in the free stream, it remains to specify these quantities at the wall. A natural and convenient choice in the context of control studies via blowing/suction at the wall is to let the wall-normal disturbance velocity take nonzero values, whereas the stream- and spanwise perturbations do not. At the wall, then,

$$v(0, t) = v_{\mathrm{w}}(t), \qquad \eta(0, t) = 0, \quad \text{and} \quad \frac{\partial v(0, t)}{\partial y} = 0,$$

where $v_{\mathrm{w}}(t)$ is the (*a priori* unknown) control function specifying the wall-normal velocity at the wall, and the homogeneous Neumann condition on $v$ is a consequence of continuity. It will prove useful to have an explicit statement to the effect that the state matches the control at the wall,

$$\mathsf{H}(v(0, t), v_{\mathrm{w}}(t)) = v(0, t) - v_{\mathrm{w}}(t) = 0.$$

The temporal framework with its concomitant assumption of a parallel boundary layer presupposes that the perturbation evolves much more rapidly than the boundary layer itself. Hence it permits the consideration of streamwise varying disturbances, which is crucial when examining three-dimensional boundary layers. While the boundary layer scaling employed by Luchini (2000) would permit the treatment of a spatially developing parabolic system, it does not allow consideration of disturbances with stream- and spanwise scales of comparable magnitude.

## 3. Optimal Control Problem

There are three essential components to the optimal control problem (Abergel and Témam, 1990; Gunzburger, 1997), two of which have already been introduced. The control is the means by which the system can be manipulated, in this case $v_{\mathrm{w}}(t)$. A description of the system is provided by the state $\boldsymbol{v}$, its behavior is constrained by (1) and its attendant boundary conditions.

The remaining element in the system is a mathematical statement of the control's objective. Here the goal is to neutralize potentially disruptive perturbations in the boundary layer, thereby increasing the extent of the laminar flow state. Furthermore, this objective is to be attained optimally, i.e., using minimal effort.

A disturbance's intensity at a given time $t = \tau$ is commonly quantified by the kinetic energy density

$$E_\tau = \frac{1}{2}\int_0^\infty (\overline{u}\cdot u + \overline{v}\cdot v + \overline{w}\cdot w)\,\mathrm{d}y = \frac{1}{2k^2}\int_0^\infty (-\overline{v}\cdot\Delta v + \overline{\eta}\cdot\eta)\,\mathrm{d}y,$$

where the overbars indicate transpose conjugate quantities. The rightmost term comes about after expressing $u$ and $w$ in terms of $v$ and $\eta$, and integrating once by parts. Provided the initial conditions for the state are normalized such that $E_0 \equiv 1$, the energy becomes synonymous with the gain or growth $G$ experienced by the perturbation. Such a normalization is applied throughout this work.

An analogous control energy density can be used to quantify the control effort. Over a specified control period $t \in [0, T]$, one has

$$C = \int_0^T (\overline{v}_\mathrm{w}\cdot v_\mathrm{w})\,\mathrm{d}t,$$

where $C$ is referred to as the control energy. For an inner product between two arbitrary complex vectors $\boldsymbol{p}$ and $\boldsymbol{q}$ defined $[\boldsymbol{p}, \boldsymbol{q}] = \int_0^T (\overline{\boldsymbol{p}}\cdot\boldsymbol{q})\,\mathrm{d}t + \text{c.c.}$ with c.c. denoting complex conjugate, $C$ is seen to be proportional to the inner product of $v_\mathrm{w}$ with itself.

Although it is possible to employ other metrics in building the cost function (a point addressed further in Section 4.3), for simplicity this work restricts itself to using the growth and control energy as just described, with one caveat. In the context of transient growth phenomena it is desirable that the control be well behaved, i.e. it should not precipitate larger increases in the perturbation kinetic energy than that experienced by the uncontrolled disturbance. It is possible to penalize any such candidate control by including a term proportional to the average growth in the cost functional.

A succinct statement of the objective is now possible: minimize the growth at the end of the control period using the least control energy possible without provoking excursions in the growth at intermediate times. Proceeding to the formulation of the cost functional for a given interval $t \in [0, T]$, this becomes

$$\mathcal{J}(\boldsymbol{v}, v_\mathrm{w}) = \zeta\, C + \chi\, E_T + \psi \int_0^T E_\tau\,\mathrm{d}\tau, \tag{2}$$

which is a real scalar quantity. The real constants $\zeta$, $\chi$, and $\psi$ serve as tunable parameters weighting the control energy, the perturbation kinetic energy at the end of the control interval, and the average perturbation kinetic energy on the interval, respectively. Provided that a particular contribution in the cost functional can be associated with undesirable behavior on the part of the control, the weights can be adjusted to penalize that element. The optimal control problem consists of finding a control $v_\mathrm{w}$, and state $\boldsymbol{v}$ which minimize $\mathcal{J}$ subject to the constraint that they satisfy (1) and its boundary conditions on the interval under consideration. An essential point is that while a global extremum of the functional is certainly desirable, the techniques used in this work only guarantee a local extremum.

In light of the difficulties inherent to the solution of constrained minimization problems, it is convenient to introduce the adjoint (or costate) variables

$$\boldsymbol{a}(y, t) = (a, b)^\mathrm{T} \quad \text{and} \quad c = c(t),$$

and write a Lagrangian functional

$$\mathcal{L}(\boldsymbol{v}, v_\mathrm{w}, \boldsymbol{a}, c) = \mathcal{J}(\boldsymbol{v}, v_\mathrm{w}) - \langle \mathsf{F}\boldsymbol{v}, \boldsymbol{a}\rangle - [\mathsf{H}, c], \tag{3}$$

where the new variables play the rôle of Lagrange multipliers enforcing the constraints. The new inner product appearing above is defined $\langle \boldsymbol{p}, \boldsymbol{q}\rangle = \int_0^T \int_0^\infty (\overline{\boldsymbol{p}}\cdot\boldsymbol{q})\,\mathrm{d}y\,\mathrm{d}t + \text{c.c.}$, ensuring that the range of the functional is the real line. Since they have not been explicitly enforced, all candidate solutions will furthermore be required to satisfy the original system's boundary conditions. The introduction of (3) replaces the original

constrained optimization problem with an equivalent but more tractable unconstrained problem: determine the control $v_\mathrm{w}$, state $\boldsymbol{v}$, and costates $\boldsymbol{a}$, $c$ which render $\mathcal{L}$ stationary, in accordance with the first-order necessary conditions for an extremal point. This is accomplished by setting to zero the directional derivative with respect to an arbitrary variation in the variable under consideration, e.g., in the case of the state,

$$\frac{\partial \mathcal{L}}{\partial \boldsymbol{v}}\delta\boldsymbol{v} = \lim_{\varepsilon\to 0}\frac{\mathcal{L}(\boldsymbol{v}+\varepsilon\delta\boldsymbol{v}, v_\mathrm{w}, \boldsymbol{a}, c) - \mathcal{L}(\boldsymbol{v}, v_\mathrm{w}, \boldsymbol{a}, c)}{\varepsilon},$$

where in contrast to the case of the constrained functional, each of $\mathcal{L}$'s arguments is considered to be an independent variable.

This requirement comes about because at an extremum point the Lagrangian's first variation with respect to each of its arguments vanishes. Setting the first variation of the Lagrangian with respect to the state variables to zero as indicated above is greatly simplified provided the adjoint under the bracket inner product, $\langle \boldsymbol{v}, \mathsf{F}^*\boldsymbol{a}\rangle$, is employed. The adjoint operator is

$$\mathsf{F}^* = \mathsf{I}\frac{\partial}{\partial t} + \Lambda^*,$$

with

$$\Lambda^* = \begin{bmatrix} \Delta^{-1}(\mathsf{C}^*\Delta + 2\mathrm{i}[\alpha U' + \beta W']\partial/\partial y) & \Delta^{-1}(\mathrm{i}\beta U' - \mathrm{i}\alpha W') \\ 0 & \mathsf{C}^* \end{bmatrix} \quad \text{and} \quad \mathsf{C}^* = \mathrm{i}\alpha U + \mathrm{i}\beta W + \frac{1}{R}\Delta.$$

The complete costate equation associated with (3) then reads

$$\mathsf{F}^*\boldsymbol{a} = \boldsymbol{s}, \quad \text{where} \quad \boldsymbol{s}(y,t) = \psi\left(\frac{1}{k^2}\Delta v(y,t)\,,\; -\frac{1}{k^2}\eta(y,t)\right)^{\mathrm{T}}. \tag{4}$$

Boundary conditions for the adjoint system are found in the successive integrations by parts from which it is obtained: homogeneous Dirichlet boundary conditions apply to $\boldsymbol{a}$, additional homogeneous Neumann conditions apply to $a$. It is noteworthy that the adjoint system propagates backwards through time. Additionally, from the $v$-equation one has

$$-\chi\frac{1}{k^2}\,\Delta v(y,T) = \Delta a(y,T) \quad \text{and} \quad c(t) = \frac{1}{R}\frac{\partial^3 a(0,t)}{\partial y^3},$$

and from the $\eta$-equation one obtains

$$\chi\frac{1}{k^2}\,\eta(y,T) = b(y,T).$$

Enforcing stationarity with respect to variations in the control, $(\partial\mathcal{L}/\partial v_\mathrm{w})\,\delta v_\mathrm{w} = 0$, yields the optimality conditions

$$\zeta v_\mathrm{w}(t) = -c(t).$$

Finally, it is immediately evident upon setting the first variation of the Lagrangian with respect to the adjoint variables to zero, $(\partial\mathcal{L}/\partial\boldsymbol{a})\,\delta\boldsymbol{a} = 0$ and $(\partial\mathcal{L}/\partial c)\,\delta c = 0$, that one recovers the constraint equations, completing the optimality system. Combining the last series of results provides an expression for the terminal conditions of the adjoint system,

$$a(y,T) = -\frac{\chi}{k^2}\,v(y,T) \quad \text{and} \quad b(y,T) = \frac{\chi}{k^2}\,\eta(y,T), \tag{5}$$

as well as a relation for the control,

$$\zeta v_\mathrm{w}(t) = -\frac{1}{R}\frac{\partial^3 a(0,t)}{\partial y^3}\,. \tag{6}$$

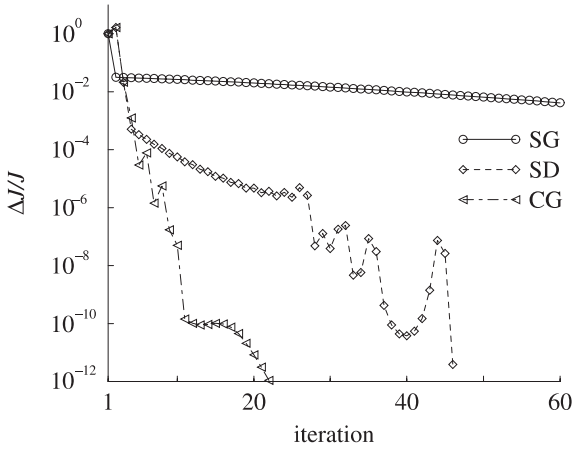


**Figure 2.** Convergence plots for different solution techniques, showing the relative change in the cost function $|\mathcal{J}^{(j)} - \mathcal{J}^{(j-1)}|/\mathcal{J}^{(j)}$ over the first 60 iterations (this quantity must be less than $10^{-10}$ for convergence). SG: simple gradient ($\varrho = 1 \times 10^{-3}$, unoptimized), SD: steepest descent, and CG: conjugate gradient.

An optimal control solution satisfies the optimality system comprising (1), with a fixed initial condition $\boldsymbol{v}_0$, (4)–(6) and minimizes (2). Implicit within the optimality system is the iterative algorithm used to solve it. Starting from an arbitrary estimate for $v_\mathrm{w}$, (1) is integrated forwards in time to $t = T$, $\boldsymbol{v}$ is stored at each step. Then (5) is used to determine terminal conditions for (4), which is subsequently integrated backwards through time to $t = 0$. Along the way the third derivative of $a$ at the wall is retained. A new estimate for the control can be obtained using

$$v_\mathrm{w}^{(j+1)} = v_\mathrm{w}^{(j)} - \varrho \left( v_\mathrm{w}^{(j)} + \frac{1}{\zeta R} \frac{\partial^3 a(0,t)}{\partial y^3} \right)^{(j)},$$

where $\varrho$ can be a constant (corresponding to a simple gradient method), or chosen to minimize the cost at each iteration $j+1$ (for a steepest descent optimization). More sophisticated solution techniques can be employed to use the functional gradient represented by $[\mathbf{1}\,,\ \zeta v_\mathrm{w} + c]$; the Polack–Ribiere variant of the standard conjugate gradient method is employed in this work (Press *et al.*, 1992). Identical results are obtained irrespective of the solution technique, but Figure 2 shows that the method selected can have a substantial effect on the computational effort. Steepest descent and conjugate gradient methods require one line minimization per iteration, implying a number of forward integrations of (1); this is unnecessary in the simple gradient method.

## 4. Results

Results are obtained using a Chebyshev collocation technique for the spatial discretization of (1) and (4) with second-order backward Euler finite-differencing for the temporal integration. The method is a generalization of that described by Corbett and Bottaro (2000), extended to treat the nonhomogeneous Dirichlet boundary conditions which apply to $\boldsymbol{v}$ and the source terms appearing in the system for $\boldsymbol{a}$. The computations presented here employ 93 collocation points with the upper boundary situated at $y_\infty = 60$, and a constant time step, $\delta t = 0.1$. Grid convergence studies show these settings are adequate to ensure well-resolved results.

As discussed by Pralits *et al.* (2001), it is possible to check that (4) has been implemented correctly by using finite differences to determine the gradient of the cost functional. For a given control $v_\mathrm{w}$ this is accomplished by setting $\hat{v}_\mathrm{w}(\tau) = v_\mathrm{w}(\tau) + \varpi$, where $\varpi$ is some small number, then integrating (1) over the interval using the modified control and evaluating $\mathcal{J}$. One then compares the output of the adjoint computation at $t = \tau$ with

$$\delta\mathcal{J}|_\tau = \frac{\partial \mathcal{J}}{\partial \hat{v}_{\mathrm{w_r}}} \delta\hat{v}_{\mathrm{w_r}} + \frac{\partial \mathcal{J}}{\partial \hat{v}_{\mathrm{w_i}}} \delta\hat{v}_{\mathrm{w_i}},$$

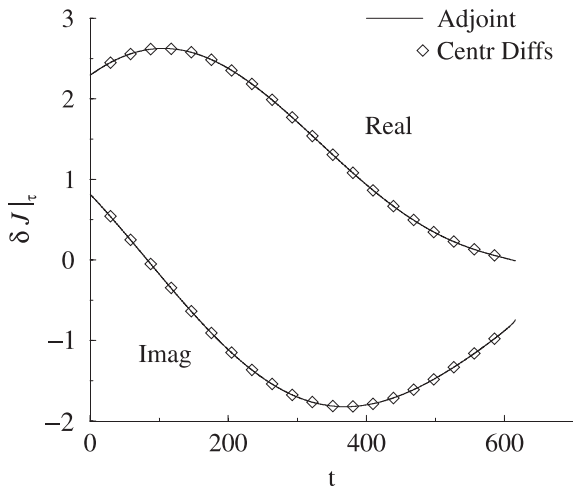


**Figure 3.** Validation of adjoint computation via centered difference evaluation of the cost functional gradient at iteration (1) : $v_w^{(1)}(t) \equiv 0$ with $\varpi = 2 \times 10^{-6}$.

where subscripts indicate the real and imaginary parts and the partial derivatives can be found using any suitable technique. Second-order centered differences have been employed to prepare the results shown in Figure 3, which compares the functional gradients for the control of a three-dimensional boundary layer. Clearly the accuracy of the procedure is a function of the time step and the magnitude of the control perturbation. Noteworthy is that each of the 20 discrete evaluations of the cost gradient corresponds to two direct integrations of (1). The advantage in carrying out instead one direct and one adjoint calculation is evident.

The discussion to follow focuses on controlling optimal perturbations in accelerated boundary layers because the rise time, i.e. , the time taken by the disturbance to attain maximum amplitude, is shortest in this type of flow. The control of optimal perturbations for three-dimensional boundary layers, which are ideally suited to precondition the flow for the exponentially amplified cross-flow instability, is particularly relevant since these experience larger transients over shorter times than their two-dimensional counterparts: they represent ideal "worst-case" scenarios for determining the feasibility of controlling rapidly varying transient phenomena. Table 1 describes the optimal perturbations experiencing the largest algebraic growth in subcritical favorable pressure-gradient flows found by Corbett and Bottaro (2001), which are investigated further below.

### 4.1. Strategy

It is unlikely that terminal control, with the sole objective of reducing the growth at the end of the optimization interval, will provide "good" results. In the context of suppressing optimal perturbations it is equally important that the control action does not induce oscillations larger than the transient one seeks to eliminate. This is expressed succinctly in (2), along with the evident desirability of employing minimal control effort; it remains to determine the magnitude of the parameters $\zeta$, $\chi$ and $\psi$ which provide satisfactory results.

Setting the optimization interval to be the characteristic rise time of the optimal perturbation for the flow under consideration (see Table 1), a set of parameters is found for which each of the elements in the cost function contributes about equally (given in Table 2 under the heading "Equil"). Now it is possible to investigate various control strategies, expressed by varying the amplitude of selected parameters. Increasing only the setting of $\zeta$ penalizes the control energy and encourages the use of minimal control effort ("cheap"). Increasing $\chi$ communicates the strong desire that the growth at the end of the interval be minimized, in this case the control energy is in effect made freely available ("small"). Raising the setting of $\psi$ restricts excursions in the instantaneous value of growth ("flat"), with a similar relaxation of the limits placed on control effort and terminal growth.

Growth curves for these cases are shown in Figure 4, where the uncontrolled case is included for reference, and circles indicate the end of the optimization interval. The disturbances' evolution is tracked beyond this point to determine their behavior after control ceases. Figure 5 shows the (spanwise-periodic)

**Table 2.** Parametric study of the effect of the scalar weights for control on the interval $T = t_\Gamma$. Given are parameter settings, value of the cost functional, control and perturbation energies.

| Case | Strategy | $\zeta$ | $\chi$ | $\psi$ | $\mathcal{J}$ | $C$ | $E_T$ | $\int E\,\mathrm{d}t$ |
|---|---|---|---|---|---|---|---|---|
| Two- | Equil | 1 | 1 | 0.001 | 51.0 | 16.9 | 19.3 | 14865.2 |
| dimen- | Cheap | 10 | 1 | 0.001 | 132.5 | 5.5 | 54.9 | 22261.1 |
| sional | Small | 1 | 10 | 0.001 | 126.2 | 41.7 | 4.6 | 38919.7 |
| | Flat | 1 | 1 | 0.01 | 173.6 | 15.4 | 25.1 | 13306.5 |
| Three- | Equil | 0.5 | 1 | 0.001 | 29.4 | 26.7 | 6.2 | 9845.8 |
| dimen- | Cheap | 5 | 1 | 0.001 | 110.2 | 13.1 | 34.0 | 10621.2 |
| sional | Small | 0.5 | 10 | 0.001 | 45.4 | 41.6 | 0.8 | 16930.3 |
| | Flat | 0.5 | 1 | 0.01 | 108.0 | 22.3 | 12.7 | 8409.3 |

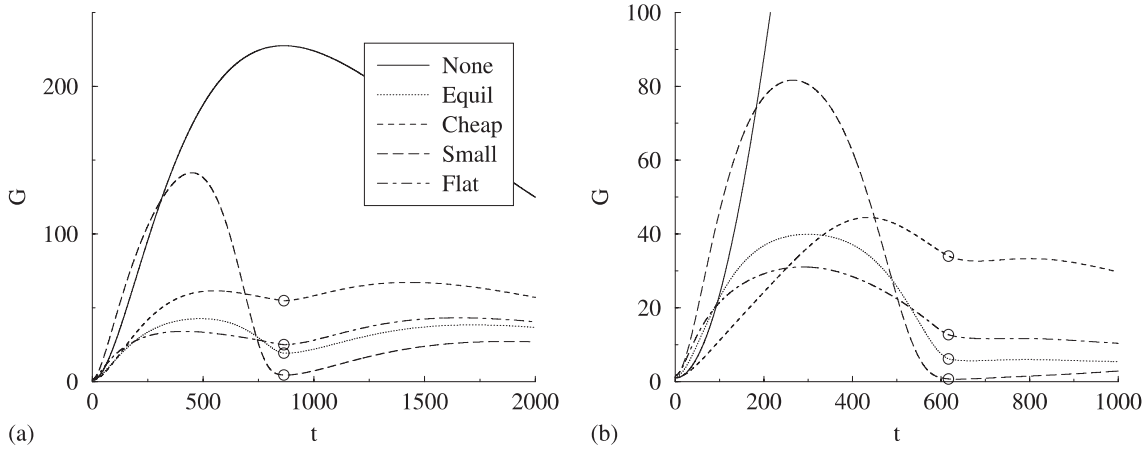


**Figure 4.** Different control strategies applied to a (a) two-dimensional and (b) three-dimensional boundary layer, with circles indicating the end of the control period, $T = t_\Gamma$.

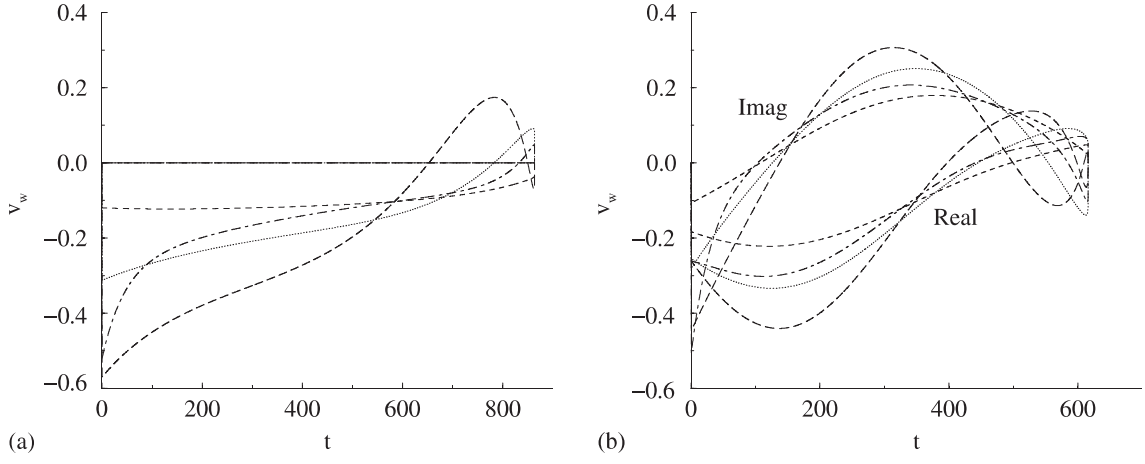


**Figure 5.** Wall velocity profiles associated with the control strategies shown in Figure 4 for a (a) two-dimensional (zero imaginary part), (b) three-dimensional boundary layer. (Line styles as in Figure 4.)

blowing/suction distribution employed in each case, the control for the three-dimensional boundary layer shows a phase lag because the optimal perturbation has nonzero streamwise wave number (see Table 1).

At first it is gratifying to note that control is generally effective in attenuating the disturbance, and that the growth as control ends is reduced to between less than 1% and one-quarter of its uncontrolled amplitude. Further inspection reveals similarities and differences between each of the strategies. A common feature for the range of parameters investigated is that the instantaneous growth attains a maximum before the end of

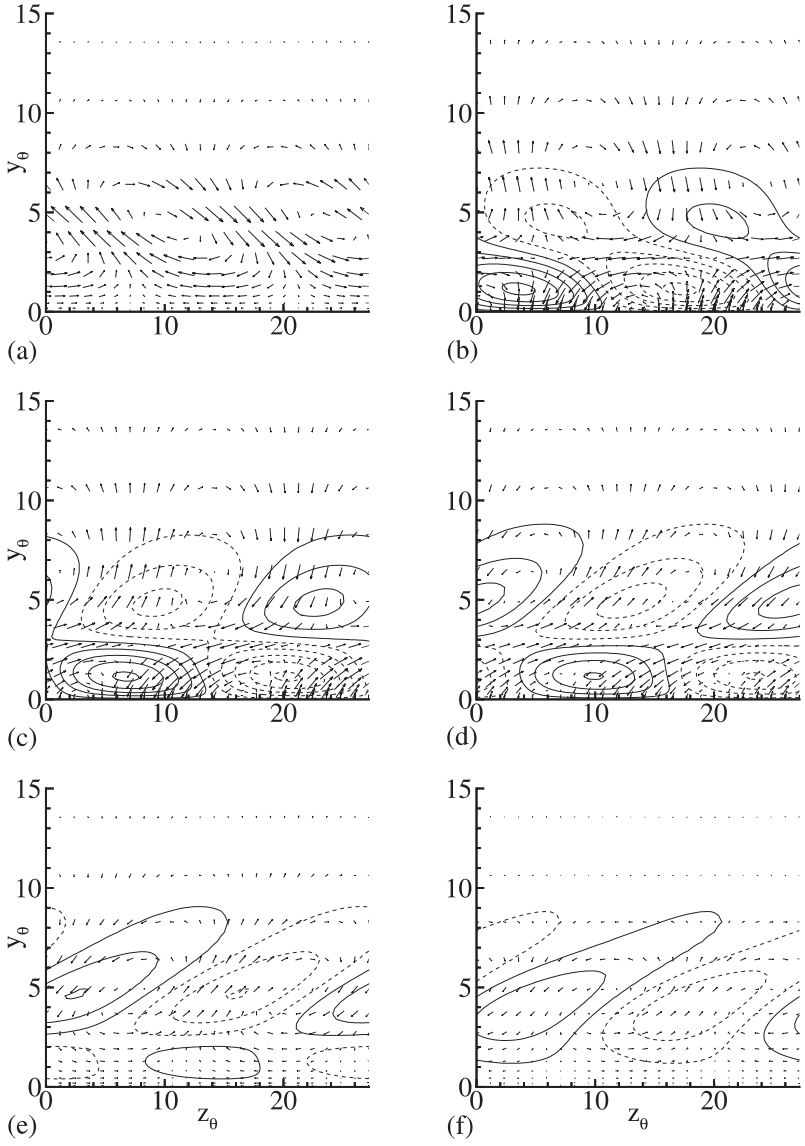


**Figure 6.** Disturbance evolution in the $y$–$z$ plane under regulation ("flat") control in a three-dimensional boundary layer at (a) $t = 0$, (b) $t = \frac{1}{4}T$, (c) $t = \frac{1}{2}T$, (d) $t = \frac{3}{4}T$, (e) $t = T$, and (f) $t = \frac{5}{4}T$, where $T = t_\Gamma$. Shown are contours of $u$ (dashed lines are negative) and a vector representation of the in-plane velocity components (vector scaling and contour levels identical in all cases).

the control span (this maximum is referred to as the excursion growth – since the ideal growth curve for the controlled flow is a straight line at unity, anything else is a deviation). Furthermore, the perturbation undergoes another transient growth phase after control ends. There is a direct correspondence between the magnitude of $E_T$ and the amount of post-control amplification (the magnitude of which is more pronounced for two-dimensional boundary layers).

When the cost functional is balanced, the second lowest values of $E_T$ and excursion growth are attained, and the growth rate is generally moderate. On the basis of terminal growth and the magnitude of the subsequent transient, "cheap" control is the least effective strategy. However, growth rates are modest and the control effort is at least a factor of two less than any other scheme; moreover, the control effort is distributed in the smoothest fashion, a consideration when seeking to apply control in an aerospace context. "Small" control achieves the smallest exit growth and consequently exhibits the smallest transient after control ceases, but this is at the expense of experiencing the largest excursion growth during the control interval, in addition to the largest growth rates. Finally, the "flat" control strategy invests most

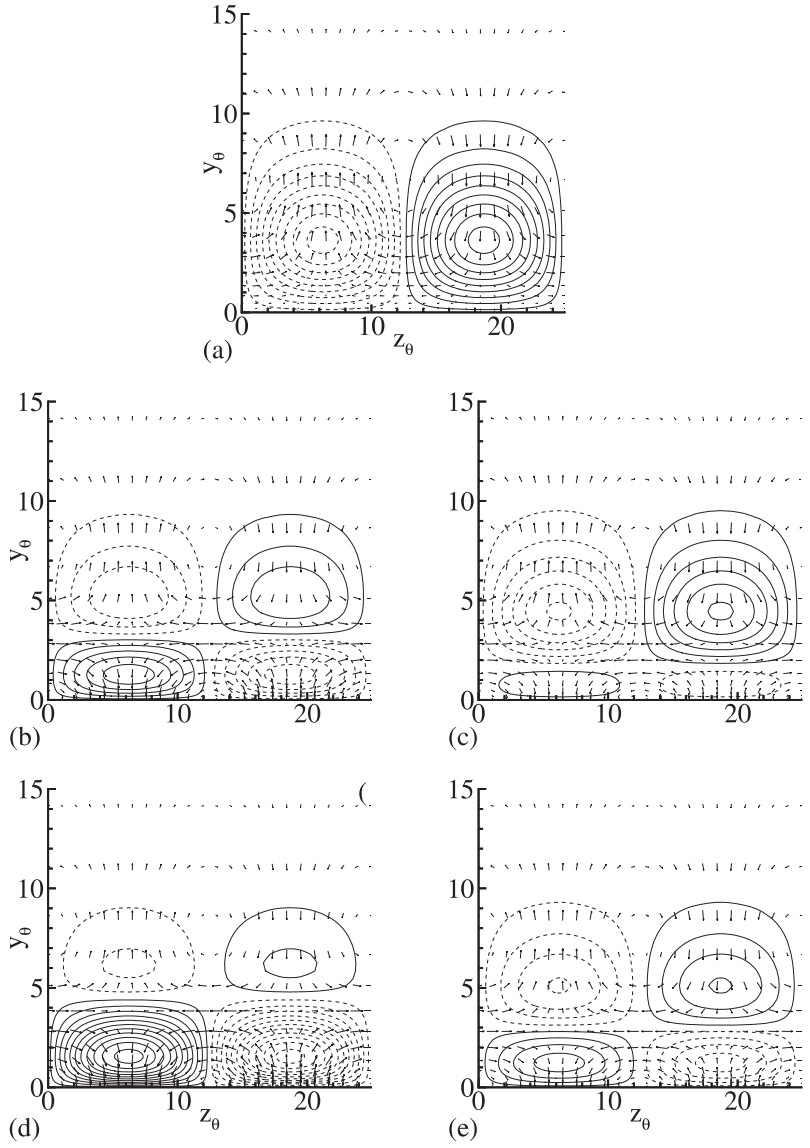


**Figure 7.** Snapshot of optimal perturbation for a two-dimensional boundary layer subject to various controls at $t = \frac{1}{2}\,T = \frac{1}{2}\,t_\Gamma$: (a) uncontrolled state for reference, (b) balanced cost control ("equil"), (c) minimal control ("cheap"), (d) terminal control ("small"), (e) regulation control ("flat"). (Vector scaling and contour levels identical in all cases.)

effort in the initial stages of the control period, and the input disturbance undergoes the least excursion growth on the interval. Note that in the two-dimensional boundary layer the output state produced by the "cheap" and "flat" strategies experiences larger post-control amplification than occurs during the optimization interval.

The physical mechanisms responsible for bringing about a reduction in perturbation kinetic energy can be inferred by studying the disturbance state as it evolves under active control. Figure 6 shows the temporal development of a disturbance subject to "flat" control in a three-dimensional boundary layer. The optimal perturbation consists of a streamwise-oriented vortex with negligible $u$-velocity component. The wall blowing/suction creates a half-vortex at the wall, in co-rotation with respect to the vortex in the free stream, which displaces the latter away from the wall and inhibits the momentum transfer from the mean flow that is the hallmark of algebraic growth. Additionally, it induces a "buffer streak" in the near-wall vicinity which supplants the principal streak created by the optimal perturbation. As confirmed by Figure 4, the key to "flat" control lies in quickly generating a buffer streak of fairly consistent magnitude. The persistent

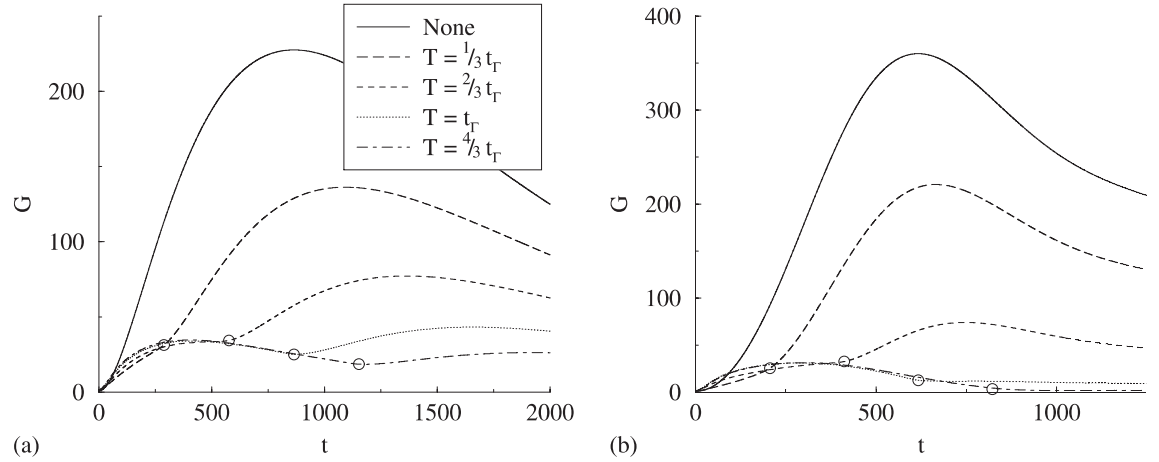


**Figure 8.** Regulation ("flat") control applied over four different time spans in a (a), and two-dimensional, (b) three-dimensional boundary layer. The end of the optimization period is shown by a circle.

crossflow-plane velocity components, although greatly attenuated in comparison with the uncontrolled case, are sufficient to sustain a long-lived weak streak after control stops.

As shown in Figure 7 for the two-dimensional boundary layer, the primary difference amongst the control strategies lies in the intensity of the buffer streak, which is proportional to the blowing/suction magnitude. This also accounts for the variations in instantaneous growth, given the more or less direct relation between the magnitude of $u$ and $E$. There is a direct link between the control effort and the displacement of the external vortex core with respect to the uncontrolled case. "Cheap" control is a good example of how small actions can result in sizeable rewards: although it changes the position of the outer streak the least it nevertheless yields a sizeable reduction in the terminal disturbance growth.

The above results indicate that optimal perturbations are remarkably difficult to control. Experiments to determine the maximum degree of suppression feasible (achieved by setting $\zeta = \chi = 0$ with some $\psi \neq 0$) produce results practically identical to those obtained using the "flat" strategy. A pronounced peak in blowing/suction as control is initiated indicates that this approach emphasizes the rapid establishment of the buffer streak.

### 4.2. Control Period

Using the characteristic time scale of the optimal perturbation is a straightforward choice for the control period: growth only occurs on this interval and the disturbance itself is in any case exponentially damped. However, there is no reason to believe that this is the best or most appropriate optimization interval. From the practical point of view it would be preferable to eliminate the threat posed by optimal perturbations as quickly as possible. The post-control transients in Figure 4 show that room for growth remains even after a prolonged intervention, so it is likely that better results will be attained for longer controls.

The "flat" strategy has been adopted in the following as its conservative approach, minimizing the disturbance activity at all times, seems most appropriate in the context of the application. Figure 8 shows growth resulting from the use of "flat" control on four optimization intervals. In each case the parameters have been tuned so that $\psi$ is ten times larger than its equilibrium value. It is apparent that for control spans less than the rise time of the optimal perturbation the disturbance is well behaved only while control is active, subsequently undergoing unacceptably large post-control amplification. So the full rise time sets a lower bound for satisfactory results, longer intervals are even better but more costly to compute. Of course the temporal framework becomes an increasingly flawed approximation as time grows large.

### 4.3. Suboptimal Control

The technological complexity of building a controller capable of precise action at an arbitrary location on the surface of a wing is formidable. More common is a series of holes or slots in the wall, as illustrated

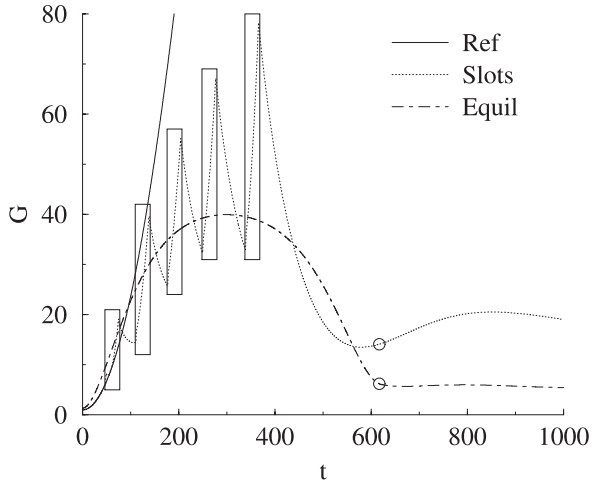


**Figure 9.** Growth resulting from application of "equil" control to a three-dimensional boundary layer on five equal intervals, simulating slots on an airfoil. The boxes indicate when blowing/suction is occurring.

in Figure 1. Provided this situation can be modeled in the temporal framework by applying control over subintervals of the optimization period it becomes possible to assess the practicability of optimal control in applications.

Figure 9 shows the result of controlling a three-dimensional boundary layer in five bursts of equal length using the "equil" strategy. Since it is evident that the boundary layer is more sensitive at small times, the control action is concentrated towards the origin. The control is switched on smoothly using a fringe function (Berlin, 1998), $f(t) = S((t-\tau_{\mathrm{on}})/\tau_{\mathrm{d}}) - S(1+(t-\tau_{\mathrm{off}})/\tau_{\mathrm{d}})$ where $\tau_{\mathrm{on}}$ and $\tau_{\mathrm{off}}$ specify the start and end times, $\tau_{\mathrm{d}}$ specifies the delay over which $f$ transitions from 0 to 1, and

$$S(\sigma) = \begin{cases} 0, & \sigma \le 0, \\ \left[1+\exp(\frac{1}{\sigma-1}+\frac{1}{\sigma})\right]^{-1}, & 0<\sigma<1\,, \\ 1, & \sigma \ge 1. \end{cases} \tag{7}$$

This is an exercise in suboptimal control since action is restricted to a portion of the optimization interval. On balance, a significant reduction in terminal growth still occurs. However, the excursion growth is on the order of the "small" strategy, and $C$ is approximately three times larger than the continuous optimal control. Inspection of the disturbance as it develops shows that the control establishes, and while active maintains, a buffer streak of fairly constant amplitude over the optimization interval.

Another challenge facing implementation of optimal control in application is that it requires full knowledge of the flow field. In practice it is rather more likely that only the flow in the immediate vicinity of a sensor can be measured, raising the interesting possibility of many actuators acting in parallel. In the temporal framework this corresponds to full knowledge on a subinterval of the whole duration of the control, and can be modeled by a normal optimization on the subinterval where the fixed input state is the output state of the preceding subinterval.

The above describes receding horizon control, another instance of suboptimal control. Applying the control strategies described in Section 4.1 in a straightforward way is tedious, since the parameters in the cost need to be adjusted such that the agglomerate cost matches the strategy.

This provides an opportunity to essay a slightly different metric in the cost functional. Define an alternative to the average kinetic energy density,

$$D = \langle \boldsymbol{v}(y,t) - \boldsymbol{r}, \boldsymbol{v}(y,t) - \boldsymbol{r} \rangle,$$

where $\boldsymbol{r} = (r_v, r_\eta)^{\mathrm{T}}$ is a fixed reference state towards which the control coerces the disturbance. Candidates include the zero vector, the initial condition (which amounts to procrastination), or a damped TS wave. The modified cost functional reads $\tilde{\mathcal{J}}(\boldsymbol{v}, v_{\mathrm{w}}) = \zeta\, C + \chi\, E_T + \mu D$. A corresponding modification to the optimality

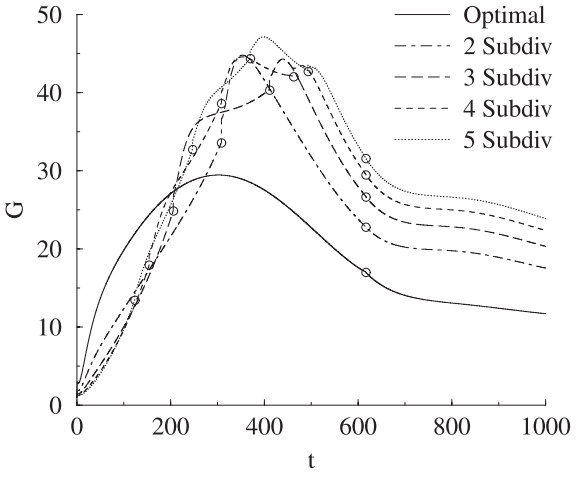


**Figure 10.** Receding horizon suboptimal control ($\zeta = 1$, $\chi = 0.1$, $\mu = 1$; $\boldsymbol{r} \equiv \mathbf{0}$) applied to a three-dimensional boundary layer, showing the departure from optimality as the number of subintervals increases (circles indicate interval boundaries, where the control may be discontinuous).

system is required: $\boldsymbol{s}$ in (4) is replaced with

$$\tilde{\boldsymbol{s}}(y,t) = -\mu(v(y,t) - r_v\,,\ \eta(y,t) - r_\eta)^{\mathrm{T}}.$$

Figure 10 shows how the growth varies as the number of subintervals increases. It is apparent that the new metric approximates the average energy quite well, optimal control is practically identical to "flat" control. (This is not surprising, given the minor difference between the average energy and $D$ when the reference vector is zero.) As the number of subintervals increases, the overall quality of the control becomes increasingly less optimal. In fact, it tends towards duplicating the "cheap" strategy, demonstrating the increasing importance of $C$ in the cost function as the interval shortens.

## 5. Summary

The optimal control problem for perturbations provoking the largest transient growth in parallel boundary layers is considered, using a direct/adjoint technique. Uncontrolled, these initial conditions, which take the form of streamwise-oriented vortices and give rise to streamwise-oriented streaks, are capable of growing two orders of magnitude in subcritical flows. They are of particular relevance in swept boundary layers in light of their strong resemblance to exponentially amplified crossflow vortices. Accelerated two- and three-dimensional boundary layer flows are investigated since transient growth develops more rapidly in these than in adverse- or zero-pressure-gradient flows. An order of magnitude reduction in disturbance growth is demonstrated for both cases, the physics behind this attenuation is described.

The cost function combines the weighted sum of the control effort, the terminal disturbance growth, and the magnitude of the average perturbation energy over the control interval. The effect of varying the weights on the contributions and the duration of the control interval (with respect to the characteristic development time of the optimal perturbation) has been investigated. It is important to limit the instantaneous growth of the perturbation rather than focusing exclusively on its value as control ends. The rise time of the optimal perturbation sets a lower limit for the optimization span, control over shorter intervals results in unacceptable post-control amplification.

Physically, the control effort is directed at the streamwise oriented vortices which constitute optimal perturbations. In essence, the vortex core is displaced away from the wall and from the regions of high shear in the mean flow which feed the disturbance via the lift-up mechanism.

This preliminary study has shown that optimal perturbations are difficult to eliminate using a transpiring wall. Although substantially attenuated, it appears impossible to prevent them from undergoing one order

of magnitude amplification using the cost function investigated herein. It is possible that more complex optimization criteria yield better results. Note that although the blowing/suction profiles are remarkably smooth, actually implementing them poses a significant technological challenge.

Before optimal control finds application in aerospace it will be necessary to study the control of three-dimensional boundary layers in the spatial framework, and to develop robust controllers using limited information about the flow. Steps in this direction have been made by Bewley and Liu (1998), Cathalifaud and Luchini (2000), and Högberg and Bewley (2001), but much work remains. The utility of such technology is evident, and of great practical interest.

## Acknowledgment

It is a pleasure to thank: Mejdi Azaïez for cheerfully sharing his time and expertise in spectral techniques; Jan Pralits for enjoyable and enlightening discussions on control, and other important things; and the participants of EuroMech "Colloquium 415 on Shear-Flow Control" (Berlin, July 2000) whose comments concerning a presentation of parts of this work inspired improvements.

## References

Abergel, F., and Témam, R. (1990). On some control problems in fluid mechanics. *Theoret. Comput. Fluid Dyn.*, **1**: 303–325.

Berlin, S. (1998) *Oblique waves in boundary layer transition*. Ph.D thesis, Department of Mechanics, Swedish Royal Institute of Technology, Stockholm.

Bewley, T.R., and Liu, S. (1995). Optimal and robust control and estimation of linear paths to transition. *J. Fluid Mech.* **365**, 305–349.

Biringen, S. (1984). Active control of transition by periodic suction-blowing. *Phys. Fluids*, **27** (6), 1345–1347.

Bower, W.W., Kegelman, J.T., Pal, A., and Meyer, G.H. (1987). A numerical study of two-dimensional instability-wave control based on the Orr-Sommerfeld equation. *Phys. Fluids*, **30** (4), 998–1004.

Breuer, K.S., Haritonidis, J.H., and Landahl, M.T. (1989). The control of transient disturbances in a flat plate boundary layer through active wall motion. *Phys. Fluids A*, **1** (3), 574–582.

Breuer, K.S., and Kuraishi, T. (1994). Transient growth in two- and three-dimensional boundary layers. *Phys. Fluids*, **6** (6), 1983–1993.

Butler, K.M., and Farrell, B.F. (1992). Three-dimensional optimal perturbations in viscous shear flow. *Phys. Fluids*, **4** (8), 1637–1650.

Cathalifaud, P., and Luchini, P. (2000). Algebraic growth in boundary layers: optimal control by blowing and suction at the wall. *Eur. J. Mech./B-Fluids*, **19**, 469–490.

Cooke, J.C. (1950). The boundary layer of a class of infinite yawed cylinders. *Proc. Cambridge Philos. Soc.*, **46**, 645–648.

Corbett, P., and Bottaro, A. (2000). Optimal perturbations for boundary layers subject to stream-wise pressure gradient. *Phys. Fluids*, **12** (1), 120–130.

Corbett, P., and Bottaro, A. (2001). Optimal linear growth in swept boundary layers. *J. Fluid Mech.*, **435**, 1–23.

Gad-el-Hak, M. (1989). Flow control. *Appl. Mech. Rev.*, **42** (10), 261–292.

Gad-el-Hak, M. (1996). Modern developments in flow control. *Appl. Mech. Rev.*, **49** (7), 365–379.

Gaster, M. (1962). A note on the relation between temporally-increasing and spatially-increasing disturbances in hydrodynamic stability. *J. Fluid Mech.*, **14**, 222–224.

Gregory, N., Stuart, J.T., and Walker, W.S. (1955). On the stability of three-dimensional boundary layers with application to the flow due to a rotating disk. *Proc. R. Soc. Ser. A*, **248**, 155–199.

Gunzburger, M.D. (1997). Introduction into mathematical aspects of flow control and optimization. In *Inverse design and optimization methods*, von Kármán Institute for Fluid Dynamics Lecture Series Number 1997-05. von Kármán Institute, Brussels, 1–20.

Hill, D.C. (1995). Adjoint systems and their role in the receptivity problem for boundary layers. *J. Fluid Mech.*, **292**, 183–204.

Högberg, M., and Bewley, T.R. (2001). Spatially compact convolution kernels for decentralized control and estimation of transition in plane channel flow. To appear in *Automatica*. 13 pages.

Joslin, R.D. (1998). Overview of laminar flow control. Technical report, NASA Langley Research Center, Hampton, VA. NASA/TP-1998-208705, available on the Web at http://techreports.larc.nasa.gov/ltrs.

Joslin, R.D., Gunzburger, M.D., Nicolaides, R.A., Erlebacher, G., and Hussaini, M.Y. (1997). Self-contained automated methodology for optimal flow control. *AIAA J.*, **35** (5), 816–824.

Ladd, D.M. (1990). Control of natural laminar instability waves on an axisymmetric body. *AIAA J.*, **28** (2), 367–369.

Lasseigne, D.G., Joslin, R.D., Jackson, T.L., and Criminale, W.O. (1999). The transient period for boundary layer disturbances. *J. Fluid Mech.*, **381**, 89–119.

Laurien, E., and Kleiser, L. (1989). Numerical simulation of boundary-layer transition and transition control. *J. Fluid Mech.*, **199**, 403–440.

Luchini, P. (2000). Reynolds-number-independent instability of the boundary layer over a flat surface: optimal perturbations. *J. Fluid Mech.*, **404**, 289–309.

Milling, R.W. (1981). Tollmien-Schlichting wave cancellation. *Phys. Fluids*, **24** (5), 979–981.
Nayfeh, A.H. (1980). Stability of three-dimensional boundary layers. *AIAA J.*, **18** (4), 406–416.
Nayfeh, A.H., and Padhye, A. (1979). Relation between temporal and spatial stability in three-dimensional flows. *AIAA J.*, **17** (10), 1084–1090.
Pralits, J.O., Airiau, C., Hanifi, A., and Henningson, D.S. (2001). Sensitivity analysis using adjoint parabolized stability equations for compressible flows. To appear in *Flow, Turb. Combust*. 26 pages.
Press, W.H., Teukolsky, S.A., Vetterling, W.T., and Flannery, B.P. (1992). *Numerical Recipes in C*, 2nd edn. Cambridge University Press, Cambridge.
Trefethen, L.N., Trefethen, A.E., Reddy, S.C., and Driscoll, T.A. (1993). Hydrodynamic stability without eigenvalues. *Science*, **261**, 578–584.